EPR forbidden transitions in NaCl:Mn^{2+} with the radiofrequency field parallel to the static field

A. Serra-Valls, C. Gago-Bousquet, and M. García-Sucre
Instituto Venezolano de Investigaciones Científicas, Centro de Física, Apartado 1827, Caracas, Venezuela
(Received 13 November 1973)

Forbidden-transitions EPR spectroscopy in the parallel-field configuration has seldom been used despite its several positive features. We have studied these transitions at X-band frequencies for the case of an orthorhombic center involving a first-neighbor Na^+ vacancy, present at room temperature in single crystals of NaCl:Mn^{2+}. In the qualitatively valid language of perturbation theory, the analyzed transitions were of the type $\Delta M = \pm 2, \pm 1$ with $\Delta m = 0, \mp 1$. Exact diagonalization of a Hamiltonian including Zeeman, crystal-field, and hyperfine terms provides the zeroth-order eigenfunctions for the first-order perturbation treatment of the quartic-crystal-field and nuclear-quadrupole terms. This allowed accurate comparison between the experimental and calculated positions of the lines for field orientations along the ⟨100⟩ and ⟨110⟩ axes, from which the small quartic-crystal-field coefficients (a and F) and the two relations linking the nuclear quadrupole coefficients were determined to be: $a = -1.0 \pm 0.3$ G, $F = 0.0 \pm 0.1$ G, and $Q_r' + Q_p' - 2Q_q' = 8.4 \pm 3.2$ G, $2Q_r' - Q_p' - Q_q' = 0.8 \pm 0.6$ G; where r, p, and q refer to crystal axes ⟨110⟩ (vacancy axis), ⟨1$\bar{1}$0⟩, and ⟨001⟩, respectively.

I. INTRODUCTION

EPR transitions with the radiofrequency field ($\vec{H}_1$) parallel to the static field ($\vec{H}$) are all of the "forbidden" type. Among the features of this field configuration one finds that the transitions $\Delta M = \pm 1$, $\Delta m = 0$, belonging to unwanted centers present in low concentration, practically disappear. This is important since the allowed spectra of such centers can be mistaken for the forbidden ones belonging to the center under study.[1] Furthermore, in the case of an orthorhombic center and for special orientations, i.e., when $\vec{H}$ is parallel to one of the crystal-field axes, the $\Delta M = \pm 1$, $\Delta m = 0$ lines are strongly forbidden, since then terms of the type $(S_z S_\pm + S_\pm S_z)$ and others which produce similar mixings of the $|M, m\rangle$'s, are brought about only by (very small) quartic-crystal-field terms. In general, most of the transitions occurring in the perpendicular-field configuration with sizable intensity are very weak in the parallel-field configuration, and therefore both types of spectra complement each other. In spite of these positive features, parallel-field transitions have been studied in a few cases,[2] and no works on alkali halides have been reported so far.

We have studied these kinds of transitions for the well-known and far-more-abundant[3] orthorhombic center in NaCl : Mn^{2+} involving a substitutional Mn^{2+} and one Na^+ vacancy in first-neighbor position.[4,5] We have used these transitions to determine the coefficients of the small quartic-crystal-field and nuclear-quadrupolar terms which are difficult or impossible to obtain from the lines of the allowed spectra.

II. EXPERIMENTAL

A reflection X-band spectrometer was used. Owing to limitations in the space available between pole pieces and in order to use 100-kHz modulation, this study requires a specially built EPR cavity, described elsewhere,[6] operating at the same frequency and with the same sensitivity as the conventional ones. In order to enhance the signal-to-noise ratio (S/N) of the forbidden lines, linear sweeps of 100 and 10 G/min were accumulated in a computer of average transients (CAT) triggered by a NMR signal.

Single crystals were grown from aqueous solution of 1.19M NaCl doped with 10^{-2} mole% $MnCl_2$ and 10^{-1} mole% NaF. The solution was kept at the controlled temperature of 68 °C. EPR spectra from these samples could be satisfactorily attributed to the two centers involving vacancies reported in Refs. 4 and 5; but in our case, at variance with the results given in Ref. 5, the Mn^{2+} ions were found to be dispersed in the crystal lattice from the beginning, and a tendency to agglomerate with time was not observed. A typical size of the sample was $0.3 \times 0.3 \times 0.7$ cm. Once the static magnetic field was oriented, the alignment of the radiofrequency field along the static field was optimized by requiring a minimal intensity of the allowed spectrum[7] (a reduction of about 1/50 was obtained). Most forbidden transitions could be observed after 100 sweeps with a $S/N \gtrsim 8$. All measurements were carried out at room temperature.

TABLE I. Crystal-field angular factors for the two orientations I and II of the orthorhombic center corresponding to the case $\vec{H} \parallel \langle 100 \rangle$, and for the three orientations III, IV, and V of the same center corresponding to $\vec{H} \parallel \langle 110 \rangle$. The angles θ and ϕ are referred to the r, p, and q crystal-field axes, where r is the vacancy axis. The values of the parameters involved are $D = 135.9 \pm 0.4$ G, $E = 51.2 \pm 0.3$ G ($g = 2.0012 \pm 0.0002$).

	g_0	$g_{\pm 1}$	$g_{\pm 2}$	Abund.
$\vec{H} \parallel \langle 100 \rangle$				
I ($\theta = 45°$, $\phi = 0°$)	$\frac{1}{4}(D+3E)$	$\frac{1}{4}(D-E)$	$\frac{1}{8}(D+3E)$	4
II ($\theta = 90°$, $\phi = 90°$)	$-\frac{1}{2}(D+3E)$	0	$\frac{1}{4}(D-E)$	2
$\vec{H} \parallel \langle 110 \rangle$				
III ($\theta = 0°$, $\phi =$ arb.)	D	0	$\frac{1}{2}E$	1
IV ($\theta = 90°$, $\phi = 0°$)	$\frac{1}{2}(-D+3E)$	0	$\frac{1}{4}(D+E)$	1
V ($\theta = 60°$, $\phi = \frac{1}{2}\cos^{-1}(-\frac{1}{3})$)	$-\frac{1}{8}(D+3E)$	$(\sqrt{3}/8)(D+\frac{1}{3}E) \mp iE/\sqrt{6}$	$\frac{1}{16}(3D-\frac{5}{3}E) \pm (i/\sqrt{18})E$	4

III. THEORETICAL

Neglecting the super-hyperfine interactions, which in our case only contribute to the linewidth, the effective spin Hamiltonian[8] is given by

$$\mathcal{H} = \mathcal{H}_0 + \mathcal{H}_{\text{quartic}} + \mathcal{H}_{\text{nuclear}} , \tag{1}$$

where, in conventional notation,

$$\mathcal{H}_0 = g\mu_B H S_z + A\vec{I}\cdot\vec{S} + g_0 S_z^2 + g_{+1}(S_z S_+ + S_+ S_z) + g_{-1}(S_z S_- + S_- S_z) + g_{+2} S_+^2 + g_{-2} S_-^2 , \tag{2}$$

in which the angular coefficients g_k are given in Table I for $\vec{H}$ along axes of the type $\langle 100 \rangle$ and $\langle 110 \rangle$. The $\mathcal{H}_{\text{quartic}}$ term represents the fourth order contribution to the crystal field and can be written in terms of well-known spin operators[9] as

$$\mathcal{H}_{\text{quartic}} = \tfrac{1}{120}\, a(O_4^0 + 5O_4^4) + \tfrac{1}{135}\, F O_4^0 + B_4^2 O_4^2 + B_4^4 O_4^4 , \tag{3}$$

where the first term is referred to the cubic axes and the other ones are referred to the rhombic crystal-field axes which are defined following the same convention as in Ref. 5. In our analysis, only the a and F terms will be considered. Expressing them in terms of the S_z and $S_\pm$ operators, and ignoring unimportant terms for the resonance, one obtains

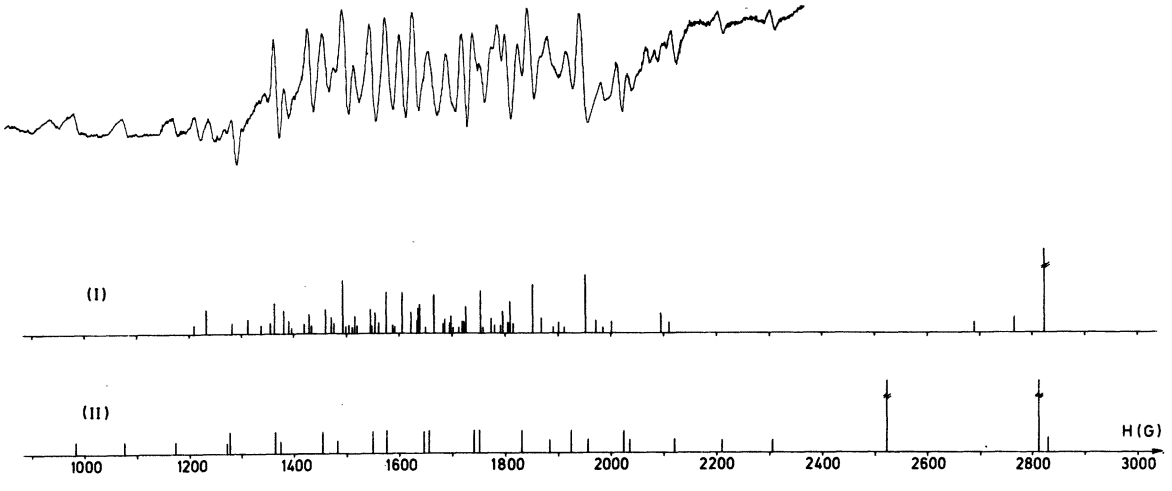

FIG. 1. Parallel-field transitions at low field of NaCl : Mn^{2+} with $\vec{H} \parallel \langle 100 \rangle$. Overlapping intervals of 240 G swept at 100 G/min were used. Relative variations in vertical scale of about 20% exist from one interval to another due to differences in the number of sweeps accumulated, which typically was 100. Theoretical spectra I and II correspond to centers with relative abundance 4 and 2, respectively. Broken vertical lines give, for reference, the position of the first allowed lines which experimentally appeared with a residual intensity comparable to that of the more intense lines at left. $\hbar\omega_K / g\mu_B = 3339.7 \pm 0.4$ G.

$$\mathcal{H}_{\text{quartic}} \simeq \tfrac{1}{24}a(1-5\Phi)(7S_z^4 - \tfrac{95}{2}S_z^2) + \tfrac{1}{144}F\{7(3-16\gamma^2+17\gamma^4)S_z^4 + 2[-2(6\vec{S}^2-5) + (46\vec{S}^2-15)\beta^2 - 7(7\vec{S}^2-5)\beta^4]S_z^2\} + \text{NDT}, \quad (4)$$

where

$$\Phi = \gamma_1^2\gamma_2^2 + \gamma_2^2\gamma_3^2 + \gamma_3^2\gamma_1^2 .$$

The γ_k's are the direction cosines of $\vec{H}$ in the system of cubic axes, and $\gamma^2 = 1-\beta^2 = \cos^2\theta$, where θ is the angle between $\vec{H}$ and the vacancy axis. NDT stands for the nondiagonal terms in the $|M, m\rangle$ basis. Their influence is generally very small, as M is found to be a good quantum number for all relevant transitions.

The quadrupolar interaction in $\mathcal{H}_{\text{nuclear}}$, Eq. (1),

TABLE II. Partial list of relatively isolated parallel-field transitions of NaCl:Mn^{2+} for the possible orientations I and II of the orthorhombic center when $\vec{H} \parallel \langle 100 \rangle$, and for the orientation III when $\vec{H} \parallel \langle 110 \rangle$. I, II, and III have relative abundance 4, 2, and 2, respectively. Two allowed transitions in the perpendicular field configuration are given as references. The cavity frequencies in gauss for $\vec{H} \parallel \langle 100 \rangle$ and $\vec{H} \parallel \langle 110 \rangle$ were 3339.7 ± 0.4 and 3320.7 ± 0.4 G, respectively. To obtain the numerical coefficients appearing in the quartic terms correction use has been made of: $M^n \approx \langle S_z^n \rangle$ (n=1, 2, 4) as a valid approximation for the lines shown in this table.

	Magnetic field position Expt. (G)	Calc.[b] (G)	Intensities Expt.[c]	Calc.	$\bar{M}$[d] / $\bar{M}'$	$\bar{m}$[d] / $\bar{m}'$	Small corrections[d,e] 1st order pert. theor.
			$\vec{H} \parallel \langle 100 \rangle$				
	1791.4 ± 0.9	1795.6 ± 0.4	0.04	0.048	1.502 / −0.504	2.488 / 1.235	$a + \frac{49}{288}F - \frac{\Delta\langle m^2\rangle}{2}q_0 + \frac{1}{2}Z_N$
	1806.9 ± 0.9	1809.8	0.09	0.070	1.502 / −0.499	2.488 / 2.001	$a + \frac{49}{288}F - \frac{\Delta\langle m^2\rangle}{2}q_0 + \frac{1}{2}Z_N$
I	1852.4 ± 0.9	1851.2	0.11	0.101	0.496 / −1.472	1.447 / 1.481	$-a - \frac{49}{288}F$
	1952.5 ± 0.9	1951.5	0.11	0.121	0.515 / −1.459	2.414 / 2.466	$-a - \frac{49}{288}F$
	1829.8 ± 0.9	1831.4	0.03	0.047	1.487 / −0.483	0.509 / 0.486	$\frac{7}{4}a + \frac{7}{8}F$
	1924.9 ± 0.9	1925.8	0.04	0.046	1.500 / −0.476	1.495 / 1.479	$\frac{7}{4}a + \frac{7}{8}F$
II	2209.1 ± 0.5	2210.8 (2212.4)	0.03	0.026 (0.029)	2.478 / 0.512	1.518 / 1.487	$\frac{7}{4}a + \frac{7}{8}F$
	2304.4 ± 1.2	2306.6 (2306.8)	0.03	0.026 (0.029)	2.496 / 0.521	2.500 / 2.479	$\frac{7}{4}a + \frac{7}{8}F$
	2522.4 ± 0.5[a]	2522.1 (2523.0)	10	9.958 (9.944)	−1.503 / −2.499	−2.494 / −2.500	...
			$\vec{H} \parallel \langle 110 \rangle$				
	2513.0 ± 0.9	2513.1	0.03	0.030	2.491 / 1.487	−1.493 / −0.490	$-\Delta\langle m^2\rangle q_0 + Z_N$
	2857.2 ± 0.5	2858.3	0.05	0.046	1.490 / 0.490	−1.492 / −0.492	$-\frac{7}{8}a + \frac{7}{3}F - \Delta\langle m^2\rangle q_0 + Z_N$
III	4125.4 ± 0.9	4126.5	0.03	0.029	−1.496 / −2.492	0.497 / 1.493	$-\Delta\langle m^2\rangle q_0 + Z_N$
	4099.0 ± 0.9[a]	4098.7	5	4.728	−1.492 / −2.494	2.494 / 2.495	...

[a] Allowed transitions (perpendicular-field configuration) included here as references.

[b] Numbers in parentheses are perturbation-theory values. The relative intensity and position of the lines were obtained using first- and second-order perturbed wave functions, respectively.

[c] The experimental intensities were taken equal to the peak-to-peak amplitudes of the envelope.

[d] $\bar{M}$, $\bar{m}$ and $\langle m^2 \rangle$ stand for the computed exact averages of S_z, I_z and I_z^2, respectively. $Z_N \equiv 0.375 \times 10^{-3}\, H\, \Delta\bar{m}$ arises from the nuclear Zeeman contribution.

[e] q_0 equals $\frac{1}{4}(Q_r' + Q_p' - 2Q_q')$ for I, and $Q_r' - \frac{1}{2}(Q_p' + Q_q')$ for III.

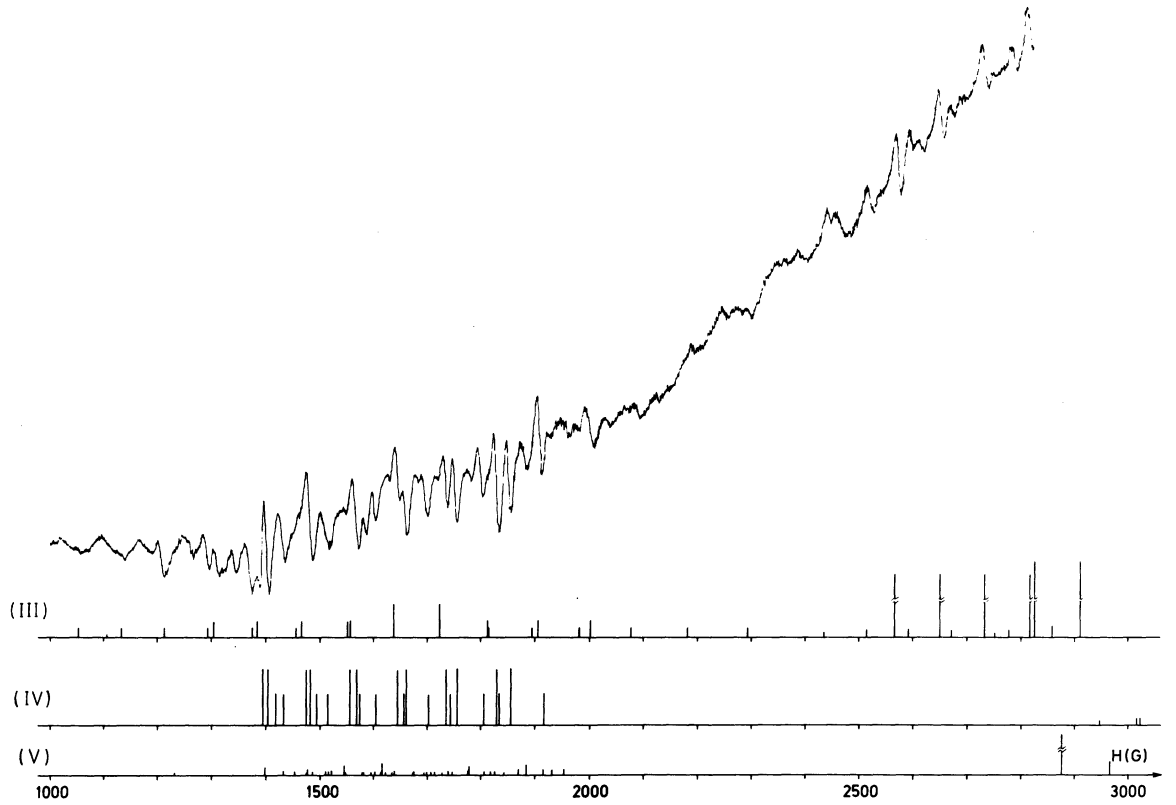

FIG. 2. Forbidden transitions of NaCl:Mn^{2+} with the radiofrequency and static fields parallel to crystal axis ⟨110⟩. Overlapping intervals of 240 G swept at 100 G/min and 100 sweeps accumulated per interval were used to reconstruct the experimental envelope. Theoretical spectra III and IV correspond to centers with their vacancy axis parallel and perpendicular to the static magnetic field, respectively (relative abundance 1). Spectrum V corresponds to the center with relative abundance 4. The slow rise of the envelope is due to the bulk of the residual allowed spectrum centered at ~3400 G. Broken vertical lines indicate the position of the first lines of this residual spectrum. $\hbar\omega_K/g\mu_B = 3320.7 \pm 0.4$ G.

can be written[8]

$$Q'_p I_p^2 + Q'_q I_q^2 + Q'_r I_r^2 \ , \tag{5}$$

where the principal axes of the quadrupolar tensor have been assumed to be parallel to the crystal-field axes.[10] Expressing Eq. (5) in terms of the operators I_z and $I_\pm$ and including the contribution of the nuclear Zeeman term, we have

$$\begin{aligned}\mathcal{H}_{\text{nuclear}} = {} & q_0 I_z^2 + q_{+1}(I_z I_+ + I_+ I_z) + q_{-1}(I_z I_- + I_- I_z) \\ & + q_{-2} I_-^2 + q_{+2} I_+^2 + g_I \mu_N H I_z \ ,\end{aligned} \tag{6}$$

where

$$q_0 = \tfrac{1}{2}(2Q'_r - Q'_p - Q'_q) - 6K(\theta, \phi) \ ,$$

$$q_{\pm 1} = 2K(\theta, \phi)\cot\theta \mp (i \sin\theta \sin 2\phi)\tfrac{1}{4}(Q'_p - Q'_q) \ ,$$

and

$$q_{\pm 2} = K(\theta, \phi) + (\cos 2\phi \pm i \cos\theta \sin 2\phi)\tfrac{1}{4}(Q'_p - Q'_q) \ ,$$

with

$$K(\theta, \phi) \equiv \sin^2\theta \tfrac{1}{4}(Q'_r - Q'_p \cos^2\phi - Q'_q \sin^2\phi) \ .$$

A computer program was used to diagonalize $\mathcal{H}_0$ in a standard $|M\rangle\ |m\rangle$ basis set. On the other hand, due to the relatively moderate importance of the crystal-field and hyperfine terms, the eigenfunctions of $\mathcal{H}_0$ obtained from perturbation theory yield a description which can be expected to be at least qualitatively valid. In fact, results from second-order (and even first-order) perturbed wave functions were frequently found to be in good agreement with the results from exact diagonalization (see Table II). However, because of the smallness of the quartic and nuclear quadrupole coefficients and because $\langle I_z \rangle$ is not always a good quantum number, the exact diagonalization results were used in computational work.

In the parallel-field configuration and using first-order perturbed wave functions, the relative intensities $|\langle M'm'|2S_x|Mm\rangle|^2$ of the main lines[11] and their selection rules are given by

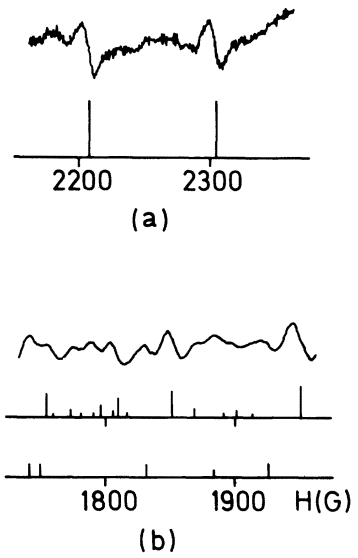

FIG. 3. Forbidden transitions of NaCl:Mn^{2+} induced by a radiofrequency field parallel to the static one, and to the ⟨100⟩ axis. Sweeps of 100 G/min in 240-G intervals were used. The number of sweeps accumulated in (a) and (b) was 80 and 172, respectively, and $\hbar\omega_K/g\mu_B = 3339.7 \pm 0.4$ G. Theoretical spectra shown below each experimental curve do not include the influence of the quartic and nuclear quadrupole terms. The small but systematic discrepancies were used to obtain the corresponding coefficients.

(a) for $M' = M \pm 1$, $m' = m$:

$$4\,\frac{|g_{+2}|^2}{(g\mu_B H)^2}\,[S(S+1) - M(M\pm 1)][2M \pm 1]^2\,, \tag{7}$$

(b) for $M' = M \pm 2$, $m' = m$:

$$4\,\frac{|g_{+1}|^2}{(g\mu_B H)^2}\,[S(S+1) - M(M\pm 1)] \times [S(S+1) - (M\pm 1)(M\pm 2)], \tag{8}$$

and (c) for $M' = M \pm 1$, $m' = m \mp 1$:

$$A^2[S(S+1) - M(M\pm 1)][I(I+1) - m(m\mp 1)]\,. \tag{9}$$

Transitions which appear in second or higher orders could be expected to be of lower intensity. However, exact diagonalization for some of these lines yields intensities which are comparable to the previous ones. In these cases, perturbation theory either fails or is unpractical.

IV. RESULTS

We have studied spectra with $\vec{H} \parallel \langle 100\rangle$ and $\vec{H} \parallel \langle 110\rangle$. The angular variation of the line positions has stationary points for these two orientations allowing a considerable reduction in the effect of misalignment errors. In our crystal, allowed spectra from the orthorhombic and tetragonal center reported in Refs. 4 and 5 were present (the tetragonal centers involve a vacancy in second-neighbor position). The orthorhombic center was found to be about eight times more abundant than the tetragonal one. The values of the crystal-field and hyperfine parameters used in the numerical calculations were determined from the extreme lines of the allowed spectra. We have found $D = 135.9 \pm 0.4$ G, $E = 51.2 \pm 0.3$ G, and $A = -90.1 \pm 0.2$ G for the orthorhombic center.

Figures 1 and 2 show transitions corresponding to $\vec{H} \parallel \langle 100\rangle$ and $\vec{H} \parallel \langle 110\rangle$, respectively. Almost all lines were satisfactorily explained as arising from the orthorhombic center. Only a few very weak lines do not seem to belong to this center and we have interpreted them as part of the more intense forbidden lines of the tetragonal center; their signals were too poor to be useful. Several of the transitions attributed to the orthorhombic center are free from overlap (see Table II and Fig. 3) and lend themselves to a straightforward comparison with the calculated results. In order to minimize the errors in the line-position determination, these lines have been also recorded at a 10-G/min rate and using a larger number of sweeps. On the other hand, owing to overlap with the bulk of the residual allowed spectrum most of the high-field forbidden lines cannot be used.

For $\vec{H} \parallel \langle 100\rangle$ two different kinds of spectra are present and the major contribution to the intensity comes from the spectrum of abundance 4 (see Table I and Fig. 1). Whereas, in the $\vec{H} \parallel \langle 110\rangle$ case the major contribution comes from the spectra of abundance 1, arising from centers having $\vec{H}$ perpendicular or parallel to the vacancy axis (Fig. 2). The observed linewidth, for allowed and forbidden lines, was slightly less than 10 G.

The numerical values of the crystal-field parameters used in the calculations were determined from the allowed spectra ignoring the presence of small quartic terms; thus the calculation of the allowed lines with these parameters essentially includes the effect of these small quartic terms (Table II). However, discrepancies associated with these terms can be expected between the experimental and calculated positions of the forbidden lines. By keeping track of the influence of the quartic and nuclear quadrupole terms [Eqs. (4) and (6)] as first-order corrections and using the position of several relatively isolated lines (Table II) one obtains[12]

$$a = -1.0 \pm 0.3 \text{ G},$$

$$F = (0.0 \pm 0.1) \text{ G},$$

$$Q_r' + Q_p' - 2Q_q' = (8.4 \pm 3.2) \text{ G},$$

and

$$2Q_r' - Q_p' - Q_q' = (0.8 \pm 0.6) \text{ G}.$$

An important feature to be taken into account in the treatment of the nuclear quadrupole corrections to the line positions arises from the fact that $\langle I_z \rangle$ often cannot be considered a good quantum number. For some of the relevant transitions differences between $\Delta\langle I_z^2 \rangle$ and $\Delta\langle I_z \rangle^2$ of the order of 15% were found.

V. CONCLUSIONS

We have presented a case in which parallel forbidden transitions give access to information not readily available in the allowed spectrum. Due to the $\Delta m = 0$ rule, this is particularly true for the nuclear quadrupole coupling coefficients which have so far remained unmeasured in spite of their relatively large value. Furthermore, the relations found between the Q' coefficients in this center indicate a quadrupolar interaction considerably larger than in the case of centers involving only chemical impurities as the source of the crystal field.[13] This suggests that a first-neighbor vacancy is a more effective source of electrostatic field gradient at the nucleus than a strong covalent coupling.

The above value for the quartic coefficient, a, agrees well with that previously reported (with some caution) by Watkins[4] on the basis of the angular variation of the allowed spectrum and ignoring a possible F term. Our measurements corroborate the rather exceptional negative sign of the a parameter and the assumption of a negligable value for F.

ACKNOWLEDGMENTS

Thanks are due to J. Serra, J. Rodríguez and F. Kaiser for technical assistance at different stages of this work.

[1] C. Gago-Bousquet, M. García-Sucre and A. Serra-Valls, Phys. Rev. B 6, 2537 (1972).

[2] The $Zn(ClO_4)_2 \cdot 6H_2O : Mn^{2+}$ system has been studied by I. J. Fritz and L. Yarmus, Phys. Rev. 173, 445 (1968); $MgO : Mn^{2+}$ by P. A. Narayana and K. V. L. N. Sastry, J. Chem. Phys. 54, 2281 (1971); and $CaCO_3 : Mn^{2+}$ by P. A. Narayana, J. Chem. Phys. 55, 4283 (1971).

[3] A ratio of 8 to 1 relative to the tetragonal center was observed in our crystals. No traces of other types of center were found.

[4] G. D. Watkins, Phys. Rev. 113, 79 (1959).

[5] K. Morigaki, M. Fujimoto, and J. Itoh, J. Phys. Soc. Jap. 13, 1174 (1958).

[6] A. Serra-Valls, C. Gago-Bousquet, and M. García-Sucre, Acta Cient. Ven. 24, (Suppl.) 27 (1973).

[7] A residual allowed spectrum is always present due to minimal errors in field parallelism and also because in a small portion of a sample of finite thickness, the lines of the $\vec{H}_1$ field are not strictly parallel to $\vec{H}$.

[8] See, e.g., A. Abragam and B. Bleaney, *Electron Paramagnetic Resonance of Transition Ions* (Clarendon, Oxford, 1970).

[9] See. e.g., M. T. Hutchings, Solid State Phys. 16, 227 (1964).

[10] That is, r refers to the vacancy axis (say the $\langle 110 \rangle$ axis) and q refers to the cubic axis perpendicular to the vacancy plane.

[11] Almost all transitions with a sizable intensity are of types (a), (b) or (c).

[12] Laplace's equation provides a third relation for the Q' coefficients, from which one obtains: $Q'_r = 0.3 \pm 0.2$ G, $Q'_p = 2.5 \pm 1.1$ G and $Q'_q = -2.8 \pm 1.1$ G. These values yield $\eta \equiv (Q'_r - Q'_p)/Q'_q = 0.8 \pm 0.2$ for the anisotropy parameter.

[13] See, for instance, K. N. Shrivastava and P. Venkateswarlu, Proc. Ind. Acad. Sci. A 63, 311 (1965) and Ref. 4.